DIGITAL ACCESS TO
SCHOLARSHIP AT HARVARD
DASH.HARVARD.EDU

HARVARD LIBRARY
Office for Scholarly Communication

Mapping the primate lateral geniculate nucleus: A review of experiments and methods

The Harvard community has made this article openly available. **Please share** how this access benefits you. Your story matters

Citation	Jeffries, Ailsa M., Nathaniel J. Killian, and John S. Pezaris. 2017. "Mapping the primate lateral geniculate nucleus: A review of experiments and methods." Journal of physiology, Paris 108 (1): 3-10. doi:10.1016/j.jphysparis.2013.10.001. http://dx.doi.org/10.1016/j.jphysparis.2013.10.001.
Published Version	doi:10.1016/j.jphysparis.2013.10.001
Citable link	http://nrs.harvard.edu/urn-3:HUL.InstRepos:33029760
Terms of Use	This article was downloaded from Harvard University's DASH repository, and is made available under the terms and conditions applicable to Other Posted Material, as set forth at http://nrs.harvard.edu/urn-3:HUL.InstRepos:dash.current.terms-of-use#LAA

Mapping the primate lateral geniculate nucleus: A review of experiments and methods

Ailsa M. Jeffries[1], **Nathaniel J. Killian**[1], and **John S. Pezaris**[*]
Department of Neurosurgery, Massachusetts General Hospital, Harvard Medical School, 55 Fruit Street, Boston, MA 02114, USA

Abstract

Mapping neuronal responses in the lateral geniculate nucleus (LGN) is key to understanding how visual information is processed in the brain. This paper focuses on our current knowledge of the dynamics the receptive field (RF) as broken down into the classical receptive field (CRF) and the extra-classical receptive field (ECRF) in primate LGN. CRFs in the LGN are known to be similar to those in the retinal ganglion cell layer in terms of both spatial and temporal characteristics, leading to the standard interpretation of the LGN as a relay center from retina to primary visual cortex. ECRFs have generally been found to be large and inhibitory, with some differences in magnitude between the magno-, parvo-, and koniocellular pathways. The specific contributions of the retina, thalamus, and visual cortex to LGN ECRF properties are presently unknown. Some reports suggest a retinal origin for extra-classical suppression based on latency arguments and other reports have suggested a thalamic origin for extra-classical suppression. This issue is complicated by the use of anesthetized animals, where cortical activity is likely to be altered. Thus further study of LGN ECRFs is warranted to reconcile these discrepancies. Producing descriptions of RF properties of LGN neurons could be enhanced by employing preferred naturalistic stimuli. Although there has been significant work in cats with natural scene stimuli and noise that statistically imitates natural scenes, we highlight a need for similar data from primates. Obtaining these data may be aided by recent advancements in experimental and analytical techniques that permit the efficient study of nonlinear RF characteristics in addition to traditional linear factors. In light of the reviewed topics, we conclude by suggesting experiments to more clearly elucidate the spatial and temporal structure of ECRFs of primate LGN neurons.

Keywords

LGN; Thalamus; Reverse correlation; Early visual system; Extra-classical receptive field

[*]Corresponding author. Address: Massachusetts General Hospital, 55 Fruit Street, THR-425, Boston, MA 02114, USA. Tel.: +1 617 643 5313. pezaris.john@mgh.harvard.edu (J.S. Pezaris).
[1]These authors contributed equally to this work.

1. Introduction

The dorsal lateral geniculate nucleus (LGN) of the thalamus is a small, bi-lateral structure that accepts input from each eye representing the contralateral half of the visual field and projects to the primary visual cortex (see Fig. 1). In higher primates, the structure comprises six laminae with associated inter-laminar structures that macroscopically segregate the magno-, parvo-, and koniocellular visual streams originating in the anatomically ipsi- and contralateral eyes. The LGN receives input that originates at the retina, passes through the optic nerves, continues to the optic chiasm where signals from the two eyes are shuffled into the two visual hemifields, then courses along the optic projection to the LGN. The LGN, in turn, sends its output along a projection to primary visual cortex (Area V1) via the optic radiation.

Cells in the LGN respond to small, well-defined regions of visual space that are called visual receptive or response fields (RFs), much like those found in the ganglion cell layer of the retina (RGC). The typical RF can be thought of as a spatio-temporal differentiator that responds best to highly local changes in visual contrast (see Fig. 2 and discussed in Section 2 below). Changes can be either spatially or temporally expressed, with cells largely falling into one of two categories, those that respond to either focal increases (*on* cells) or decreases (*off* cells) of luminance. There is nearly a one-to-one anatomical mapping from retina to LGN in the cat (Hamos et al., 1987) and evidence for similarly high anatomical specificity in primates (Conley and Fitzpatrick, 1989). In addition, there is a nearly one-to-one functional mapping in cats (Cleland et al., 1971) and primates (Kaplan et al., 1987; Lee et al., 1983; Sincich et al., 2009b) from ganglion cell output to LGN cell input, so the close matching of RF characteristics between RGCs and LGN neurons is perhaps not surprising. And, like those found in RGCs, responses in LGN are adapted by luminance and contrast at a larger spatial scale than the RF.

The standard conceptual framework that partitions visual receptive fields into a smaller classical receptive field (CRF) and a larger modulatory extra-classical receptive fields (ECRFs) was established by Hubel and Wiesel (Hubel and Wiesel, 1962, 1961, 1959) a half-century ago. In this paper we will use RF to indicate the entirety of the response field in all of its aspects, CRF to indicate just the classical, small center-surround structure, and ECRF for any parts of the RF that extend beyond the CRF in either space or time, reflecting common usage in the literature.

In this paper we review recent CRF/ECRF studies of the lateral geniculate nucleus of the thalamus. The focus of this review is on the primate LGN and we will frequently cite studies in other species such as cats that serve as points of reference for work in primates. With a growing body of knowledge about RFs in the primate early visual pathway, it is now clear that the ECRF is an important part of LGN RFs in primate, and that the functional impact of the LGN ECRF may be important for subsequent processing (Webb et al., 2005; Angelucci and Bressloff, 2006). The strength and source of the ECRF in LGN neurons is less clear — although ECRFs can be identified in RGCs, additional processing within the LGN, including feedback from cortical areas, may also be important. In the present work, we review some of the studies that have been successful at defining CRFs and/or ECRFs in the LGN. As many

of the reported results hinge upon stimulus choice, a second topic of review in this paper is the stimuli used to map LGN responses, in particular natural scenes and noise that statistically imitates natural scenes (often called 1/f noise as its power spectrum mimics that of natural scenes, although it lacks phase information that characterizes shapes in natural scenes). Using natural stimuli is important in a neuroethological context, especially if the aim is translational as clinical tools that interact with the LGN may need to do so in a natural environment (Bourkiza et al., 2013; Pezaris and Eskandar, 2009; Pezaris and Reid, 2007). A variety of methods have been used in the studies included here; we will, in particular, examine the different animal models (i.e. cat and monkey) used and touch upon the resulting biases that may exist in the literature. Hubel and Wiesel's original work was with both cats and primates, but much of the later work in the field has been done only in cats. While the cat visual system has proven to be a robust and capable experimental model, there are some fundamental differences between cat and primate visual pathways which make comparative studies important. Significant work with naturalistic stimuli (e.g. natural scenes and 1/f noise) has been performed in the cat LGN (Butts et al., 2007; Lesica and Stanley, 2004; Simoncelli and Olshausen, 2001; Stanley et al., 1999), but natural scene statistics have rarely been employed in studying the primate visual system. We conclude the review by highlighting a need for further experiments to detail RF properties of LGN with an emphasis on using the alert primate preparation.

2. Fundamental RF characteristics of the LGN

Early studies established that RFs have extent in both space and time, and thus a complete characterization requires spatio-temporal information. This realization led to the eventual application of white noise analysis and reverse correlation, derived from linear systems analysis, for the generation of accurate neuronal RF maps (DeAngelis et al., 1995). The groundbreaking work of Kuffler followed by Hubel and Wiesel determined the basic characteristics of CRFs in the retina and the LGN (Hubel and Wiesel, 1961; Kuffler, 1953), demonstrating an approximately circular center/surround organization. They described *on*-center cells, neurons that have increased firing when bright stimuli are placed in center of the RF and *off*-center cells, neurons that have increased firing when relatively dark stimuli are placed in center of the RF (see Fig. 2). Insightfully, Kuffler also described the presence of factors that were indirectly involved in RGC output, perhaps the earliest mention of ECRF-like effects, factors that "may well involve areas which are somewhat remote from a ganglion cell and by themselves do not setup discharges" (Kuffler, 1953).

Nevertheless, the fundamental characteristics of receptive fields have been substantially refined by later investigation. Some LGN cells are achromatic, responding only to luminous intensity, while others are modulated by specific colors, typically classified as belonging to one of three wavelengths: short, medium and long (Wiesel and Hubel, 1966). Later work has shown a rich set of color- opponent pairs in CRFs (Reid and Shapley, 2002). We refer the reader to Solomon and Lennie for a review of color vision physiology (Solomon and Lennie, 2007). Selectivity for long wavelengths in the LGN is most common, in agreement with the large number of cones that are selective for long wavelengths (Wiesel and Hubel, 1966). Krüger determined that color-specific cells made up 90% of the population (Krüger, 1977).

Most cells displayed these characteristics when the stimulus was larger than the receptive field.

3. Functional pathways across primates

The visual path is segregated into three major divisions at the LGN, magnocellular (M), parvocellular (P), and koniocellular (K), with functional differences between divisions largely consistent across species (Derrington and Lennie, 1984; O'Keefe et al., 1998; Usrey and Reid, 2000; White et al., 2001; Xu et al., 2001). M cells are typically achromatic, respond to higher temporal frequencies, and have large CRF centers. P cells have color-opponent structure in primates with input from two cone classes at middle and long wavelengths (Jacobs, 2008), respond to lower temporal frequencies, and have small CRF centers. Most K cells that have been described have strong input from short wavelength cones and have blue-*on* or blue-*off* CRF structure (Hendry and Reid, 2000; Martin et al., 1997; Tailby et al., 2008). According to Xu et al., a much larger portion of K cells, 34%, cannot be driven by drifting gratings, compared to only 9% of M cells and 6% of P cells (Xu et al., 2001). Recent work in primates has shown the presence of K cells with orientation selectivity that might help explain the findings of weak responses to grating stimuli (Cheong et al., 2013). K cell characteristics also vary across K layers, suggesting that there might be several classes of K cells, and appear to be more heterogeneous across species (Hendry and Reid, 2000). Xu and colleagues, as well as O'Keefe et al. (1998), looked only at owl monkeys but their combined findings agree with what Usrey and Reid found in both owl and squirrel monkeys, and with what Norton and Casagrande found in the pro-simian galago (Norton and Casagrande, 1982). Both Xu et al. and Usrey and Reid's studies found that spatial summation was linear for all LGN cells that fit the linearity-testing criterion of responding well to drifting gratings (subsequently some of the recorded K cells were not tested for linearity). Xu et al. focused on the properties of K cells while O'Keefe et al. and Usrey and Reid looked primarily at M and P cell properties. The characteristics of M and P cells that O'Keefe et al. found in owl monkeys, and Usrey and Reid found in owl and squirrel monkeys are consistent with what characteristics Maunsell et al. found in macaques (Maunsell et al., 1999). In all three species, M cells respond faster than P cells, suggesting that the division of pathways serves the same function: M cells encode spatial information and P cells encode color information. The only difference that Usrey and Reid found between owl and squirrel monkeys was that overall, visual responses in owl monkeys were slower, which they speculated may be due to the nocturnal nature of the species. Between owl and squirrel monkeys, the receptive field surrounds were equally strong for M and P neurons. Based on these studies, it appears there are more similarities than differences between primate species in the early visual system, although a full, detailed analysis is beyond the scope of the present work.

4. ECRF characteristics and the origin of ECI

Compared to the CRF, less is known about the presence of an ECRF in the primate LGN. Indirect inhibitory input to the thalamus has been shown by Babadi and colleagues to modulate LGN responses in cats (Babadi et al., 2010). By identifying retinal input through S-potentials, they were able to exclude the retina as the source of the inhibitory modulation

they observed, suggesting a non-retinal source as a likely candidate for extra-classical suppression. This agrees with the findings of Kaplan et al. (Kaplan et al., 1987), who described nonlinear contrast gain control in both the cat and monkey LGN through simultaneous S-potential and LGN single unit recordings (i.e. the retinal input could not explain the nonlinear pattern in the LGN output). Solomon, White and Martin (Solomon et al., 2002) looked extensively at the suppressive effects of ECRF stimulation, or extra-classical inhibition (ECI), in the primate LGN and found that more was present in the M and K pathways than the P pathway. Interestingly, while the strength of ECI increased as contrast increased in the ECRF, it also showed a dependence on the contrast of the RF, supporting their speculation that the ECRF might extend through the CRF as well. They suggested LGN interneurons as a likely source of ECI.

Webb and colleagues investigated the spatial distribution, both fine and coarse, of the ECRF for M and P cells (Webb et al., 2005). Their findings show that the ECRF is larger than the CRF, consistent with other reports (Alitto and Usrey, 2008; Solomon et al., 2002), but found that the ECRF is often asymmetric, concluding that there is no systematic spatial distribution to the ECRF. Webb et al. agree with Solomon et al. in the suggestion that the ECRF has different sources than the CRF, e.g. different retinal or thalamic sources, citing the correspondence between varying spatial configurations of LGN interneuron receptive fields and the asymmetric nature of ECI to also hypothesize that thalamic interneurons are involved in the ECRF. In contrast, Alitto and Usrey (2008) suggest that ECI arises too quickly after visual stimulation for its source to be cortical feedback and thus conclude it must result from feedforward suppression from the retina. In their study, the level of response suppression in the LGN was found to be similar to the level found in the retina, confirming previous observations that the characteristics of extra-classical inhibitory effects in the retina are similar to those in LGN (Solomon et al., 2006). Like in the LGN (Solomon et al., 2002), only retinal ganglion M cells, and not P, have an extra-classical surround present, with greater suppression at higher contrasts. This surround must be from ECRF activity and not CRF activity because it was found to occur in response to stimuli that had not elicited a response in the CRF (Solomon et al., 2006). Another study concluded that ECI may originate in the retina because contrast adaptation in the LGN was not tuned to orientation, spatial frequency, or temporal frequency, which would not be expected if the suppression originated in the visual cortex (Camp et al., 2009).

While there are convincing arguments for both LGN interneurons and retinal ganglion cells as ECRF sources, there may be also as-yet unobserved influences from corticothalamic feedback. Most studies have been performed with an anesthetized preparation, with therefore reduced levels of cortical activity (Haider et al., 2013; Lamme et al., 1998; Niell and Stryker, 2010) thereby presumably reducing the level of corticothalamic input and effect. In addition, the timescale of cortical influence on thalamic activity may be longer than what has been investigated, especially for anesthetized preparations (Uhl et al., 1980), or may be evident only in transient stimuli. The effect may alternately be too subtle to have been found easily, or a vital input to LGN may have been missing, like attention as seen in human fMRI by O'Connor et al. (2002), or other behaviorally driven action, like eye motion as seen in peri-saccadic influences on thalamic activity by Reppas et al. (2002). The current evidence suggests that corticothalamic feedback does not contribute to extra-classical

suppression but the possibility of an excitatory extra-classical influence remains. The presence of extra-classical suppression was found in geniculocortical afferents of anesthetized primates with a muscimol-inactivated visual cortex (Sceniak et al., 2006). Another study has compared surround suppression observed in anesthetized and alert primates and found that anesthesia does not reduce suppression (Alitto and Usrey, 2008). While Alitto and Usrey made only a qualitative comparison of the two conditions, their results suggest that suppression is actually greater in anesthetized primates. With evidence of excitatory ECRFs in V1 (Fitzpatrick, 2000) the effects of which could be communicated through the cortico-thalamic projection, we might expect to see globally balanced excitation and inhibition from the full-voiced influence of the awake cortex. One report did in fact describe weakened EC suppression following ablation of V1 in primates, suggesting that excitatory V1 feedback may somehow be balanced by other inhibitory input to LGN neurons (Webb et al., 2002).

Two different functions have been proposed for the role of the ECRF (Mante et al., 2008; Solomon et al., 2002). Firstly, the inhibitory effects from the ECRF may be the source of contrast gain control in relay cells within LGN, which could also account for the contrast-dependent nature of retinogeniculate transmission rates (Bonin et al., 2005). Secondly, ECI may lead to contrast-dependent aperture tuning, as also seen in V1 (Sceniak et al., 1999). As contrast increases, the summation field of LGN and V1 cells decreases in extent, and thus becomes more spatially localized. Interestingly, P cells, as primary input to the temporal visual pathway or *what* stream (Goodale and Milner, 1992; Ungerleider and Mishkin, 1982), do not exhibit ECRF-driven inhibition; precise spatial localization is less necessary in determining identity features. Following parallel reasoning, M cells, as primary input to the parietal *where* stream, exhibit strong extra-classical inhibition; contrast-dependent aperture tuning allows for improved spatial precision under more ideal viewing conditions.

5. Natural stimuli and LGN responses

The studies done to define primate CRFs and ECRFs have used artificial stimuli, leaving the question hanging of whether RF properties change when more naturalistic stimuli are used. Some investigators have addressed this question with intriguing results, but all of the work has been done in the cat model, as briefly summarized in the next few paragraphs.

In a classic paper studying the responses of cat LGN neurons to natural scenes, Stanley et al. (1999) mapped the CRF of 177 cells using white noise stimuli, then recorded the neural responses to three different natural scene movies, and finally performed a video reconstruction by convolving the computed CRFs with the spike trains corresponding to the natural stimuli. The results were fuzzy but recognizable reproductions of the original movies, with the distribution of per-pixel correlation between the two videos peaking at 0.6–0.7, demonstrating that RFs from white noise stimuli were at least similar to those expected from natural scenes. Building on that work, Lesica and Stanley (2004) examined the difference in tonic and burst spiking in responses to natural scene movies. Responses were predicted using an integrate-and-fire framework and then compared with observed responses, with the finding that there was more bursting in response to the natural scene movies than to the white noise. Bursting was especially strong when a long inhibitory

stimulus preceded an excitatory stimulus moving into the receptive field; moreover, bursting was found to represent a nonlinear component of the response. The more robust LGN responses to natural scenes indicate that white noise stimuli may not be as desirable when mapping RFs, especially when investigating more subtle or nonlinear effects. Further support for this idea comes from work by Talebi and Baker in a downstream part of the visual system, cat Area 18, comparing the predictive robustness of RFs generated from artificial and natural stimuli (Talebi and Baker, 2012). They recorded neuronal responses to white noise, short bars, and natural images. RF models generated from each were tested for predictive accuracy with matching-type and cross-type stimuli. White noise stimuli elicited weak neural responses, resulting in noisy models, whereas bars and natural images elicited stronger responses and more accurate models. Natural image based models performed better in cross-type validation than models from the two artificial stimuli, again suggesting that artificial stimuli may be poor probes for RF mapping.

Tan and Yao examined the power spectra of natural scenes, and found that LGN neurons have spatio-temporal frequency tuning that acts as an optimal linear filter to maximize information transmission of natural scenes (Tan and Yao, 2009). They found that the power spectra vary significantly across different scenes and speculated that the spatiotemporal frequency characteristics of LGN neurons may be tuned to the frequencies of largest variability in natural scene spectra in order to assist in discrimination of natural stimuli.

Mante et al. proposed a model which, using the same parameters that apply to simple stimuli, predicts most of the firing rate responses to complex stimuli like natural scenes (Mante et al., 2008), including an important role for ECRF suppression in contrast gain control. They combined a standard center-surround CRF with fast-adapting gain control factors driven by local luminance and local contrast in the ECRF, and found excellent predictive power for the model, except for bursting.

For further information on the topic of natural scenes, we refer the reader to Simoncelli and Olshausen (2001) review on the statistical methods available to analyze natural scene responses. They present an in-depth discussion of the efficient coding hypothesis and its applications, including single and multiple neuron encoding. Simoncelli also offers a concise review of natural scene statistics (Simoncelli, 2003), including more efficient coding hypothesis discussion that includes some criticisms of the method and proposals of how to experimentally test its validity.

6. Experimental techniques and analysis methods

Much of the early work in RF mapping used drifting bars or gratings with analysis techniques such as static maps created by line-weighting functions (Baker and Cynader, 1986; Field and Tolhurst, 1986) and response-plane maps (Palmer and Davis, 1981; Stevens and Gerstein, 1976). More recently the techniques of reverse correlation (Ringach and Shapley, 2004) driven by white noise (Chichilnisky, 2001) or M-sequence (Reid et al., 1997; Sutter, 1991) visual stimuli to map and analyze receptive fields have been developed. A typical mapping paradigm is shown in Fig. 3 where a black-and-white checkerboard stimulus is presented over a putative RF location in the visual field while neural responses

are recorded. The typical analysis that goes along with these stimuli is shown in Fig. 4 where a spike-triggered average (STA) is created by taking the mean of the instantaneous frames present at each observed spike. When the stimuli are spectrally white, and the STA is generalized to taking the average for multiple frame delays prior to each spike, the computation becomes equivalent to determining the average preferred stimulus of a given neuron, or the first order Weiner kernel (Marmarelis and Marmarelis, 1978; Victor and Knight, 1979) and thus is a description of the linear part of the neuron's transfer function.

The requirement for spectral whiteness is met by the use of carefully-constructed stimuli such as M-sequences that have been used to map RFs in the primate retina (Benardete and Kaplan, 1997a, 1997b), LGN (Reid and Shapley, 2002; Usrey and Reid, 2000), V1 (Cottaris and De Valois, 1998), and higher order visual areas (Bair et al., 2002). In the primate LGN in particular, Reid and Shapley (2002) used M-sequences to investigate functional differences between cell types in the different LGN laminae, including examining the specific retinal cone contribution to thalamic responses by shifting the black-and-white luminance axis in their checkerboards to cone-isolating colors. They found that M cell responses were transient, red-green P cell responses were relatively sustained, and blue K cell responses were the most sustained (Reid and Shapley, 2002). Although in cats rather than monkeys, Reid et al. (1997) also performed a similar experiment to examine the linear receptive field properties of Y cells with high temporal resolution.

Most M and P cells in the primate LGN have linear firing properties that can be explained by linearly weighting the stimulus light pattern by a CRF map (see Fig. 2), however, as described in Section 4, nonlinear properties such as EC suppression of M cells have been found. These nonlinear RF properties can be examined using spike-triggered covariance (STC) analysis. Solomon et al. (2010) used flickering uniform fields to stimulate primate LGN neurons, and STAs and STCs to derive estimates of the linear and second-order nonlinear receptive fields. The authors arrived at the interesting conclusion that there is a class of nonlinear cells in the LGN that encode contrast energy. Thus future investigations will benefit from taking into account nonlinearities in experimental design and analysis.

Chichilnisky presents an analysis of the advantages and disadvantages of random white noise stimuli (Chichilnisky, 2001). The benefits include minimizing the effects of adaptation, the ability to compute model-free linear responses easily, and model-free nonlinear ones with sufficient data, or, by the inclusion of a simple model, the ability to compute standard nonlinear responses quickly. While M-sequences have exact statistics when presented in entirety, they produce artifact-laden results if the sequence is not completed (Chichilnisky, 2001); moreover if a stimulus is repeated, in general, LGN responses will be almost exactly the same for each presentation (Reinagel and Reid, 2000) and thus repeating an M-sequence to extend data collection does not serve to refine measurements appreciably as the stimuli are not independent and LGN responses are precise. In contrast, random noise has more flexibility in stimulus duration, as indefinitely long stimuli can be pre-computed, arbitrary segments of which can be shown during data collection without adversely affecting stimuli statistics.

In contrast, Sincich et al. (2009a) found that neither correlated Gaussian nor random white noise were as effective at driving neurons as luminance flicker that resembled natural scene temporal fluctuations with 1/f properties. Their observations suggest that work using other and currently more common noise techniques could be sampling a limited portion of the neuronal response range.

Methodological advances have brought about the possibility of independently stimulating single retinal photoreceptors for extraordinarily fine-grained control over retinal input to LGN. McMahon et al. (2000) showed that retinothalamic circuitry can be probed in monkeys using a clever laser interferometry technique that bypasses the optics of the eye to form grating stimuli directly on the retina. In a similarly technically impressive effort, Sincich et al. (2009b) were able to reliably evoke activity from macaque LGN cells by stimulating single retinal cone cells using micron-scale spots of light targeted at the LGN CRF center with a scanning laser stimulus. Although neither study explored the ECRF, both were able to quantify the contribution of each of multiple cones spanning the CRF for a set of example thalamic cells. As the technique of adaptive optics is relatively new, we might well expect to see additional, high-input precision visual mapping results in the near future, as suggested in the recent review by Roorda (2011).

Recent technical advances have included progress in analytical methods as well. Fairhall et al. (2012) discuss recent advances in information theory such as Maximally Informative Dimensions (MID). MID allows for the use of reverse correlation techniques with stimuli other than Gaussian white noise. It also allows for the estimation of feature selectivity when natural stimuli are used. Sharpee's review (Sharpee, 2013) discusses the various models that exist to define the receptive field, specifically for use in conjunction with natural stimuli. The review is a good resource for information on linear models and their expansions, STAs, STCs, MIDs, multidimensional feature selectivity, maximally informative subspace, and maximally informative quadratic models, as well as all of these models' best suited applications and the assumptions that go along with each. These methods are particularly useful for relating neural responses even when many stages of nonlinear processing are involved. In the future, such methods could be applied to higher order visual areas where responses have complex, and sometimes unknown, invariances that characterize neural feature selectivity.

7. Proposed experiments

Combining the information presented here thus far reveals a gap in current knowledge of ECRFs in the primate LGN. The work that has been done in cats shows that natural scenes and 1/f noise are better at revealing nonlinearities in neuronal responses than white noise. Moreover, a commonly proposed model of ECRF effect is nonlinear, underscoring the potential importance of method selection. However, there is currently a lack of work in primates to examine these issues.

The cat visual system, although similar to the primate visual system, has significant differences that should give pause when generalizing findings in cats to those for primates, especially when looking for the potential influence of corticothalamic feedback. Inter-

species differences can be found at the molecular level, such as when Levitt and colleagues compared neuronal properties in visually- deprived macaques (Levitt et al., 2001), in an attempt to extend Guimaraes et al.'s previous study in cats (Guimaraes et al., 1990). Levitt et al. sutured one eye shut shortly after birth in five macaques and compared anatomical and functional differences with four macaques which had been reared with normal vision in both eyes. The authors found that immunoreactivity for a monoclonal antibody that labels magnocellular laminae (Cat-301) was uniformly reduced in laminae corresponding to the deprived eye. In cats, the Cat-301 antibody specifically labels Y cells, which are lost after deprivation (Guimaraes et al., 1990). This result provides structural evidence to suggest that primates do not possess a visual pathway strictly analogous to the Y cell pathway of cats, as had been earlier asserted by Shapley and Perry based on functional characteristics alone (Shapley and Perry, 1986).

Differences are also evident at the systems level in the early visual stream. In the cat, LGN projects to two areas of the visual cortex, Brodmann Areas 17 and 18, unlike the single projection to visual cortex in primates. Lesioning either one of Area 17 or 18 has limited effect on the functioning of the unlesioned area, and specifically does not induce profound blindness (Dreher and Cottee, 1975). In primates, the LGN projects almost solely to V1 and lesions of that area eliminate conscious sight entirely in the affected part of the visual field (Brindley et al., 1969).

In addition to the problems of generalizing across species, almost all work classifying RFs and ECRFs has been done in anesthetized animals, cats and primates alike, with some important exceptions. Alitto et al. examined the differences in visual responses of alert and anesthetized macaques (Alitto et al., 2011). They found that LGN neurons in alert animals responded with higher firing rates and the neurons had an increased ability to follow stimuli drifting at higher spatial and temporal frequencies. Moreover Reppas, Usrey and Reid (Reppas et al., 2002) found saccadic eye movements modulated LGN responses to flickering fields of uniform intensity in awake, behaving macaques. In a similar study, Saul (Saul, 2010) found that saccades changed the response times of neurons. These results show that anesthetizing the animal changes the nature of neuronal responses, especially how they might respond to natural scenes and naturalistic noise.

In a similar technical convention that has constrained results, nearly all experiments have used annular stimuli (Alitto and Usrey, 2008; Babadi et al., 2010; Solomon et al., 2006, 2002) with a limited ability to fully examine the detailed spatial structure and extent of the ECRF. Non-uniformity of an annular structure in the ECRF has been reported (Webb et al., 2005), but a rigorous, definitive mapping has not yet been performed. Contemporary stimulus generation systems are able to present full-field arbitrary stimuli at high refresh rates, and contemporary computers are readily capable of analyzing large volumes of data (Alivisatos et al., 2012; Briggman and Bock, 2012) created by extensive stochastic stimuli. Further experiments in alert primates responding to natural stimuli that address these gaps in the current body of work are needed to better understand the visual system and its properties, and the technical and analytic tools to do so are now available.

8. Conclusion

In this paper we have gathered current knowledge of primate LGN receptive fields, classical and extra-classical, to illuminate the areas that need more work to achieve a better understanding. Much less is known about ECRFs, their source, shape, and how they behave in response to stimuli, than CRFs. Most of the studies that have involved LGN mapping concentrate on the CRF, and few have examined the ECRF. Just as there is more known about CRFs than ECRFs, there is more work done using artificial stimuli than with natural stimuli. Because most of the work done has been with artificial stimuli, it is hard to know if the field is inadvertently missing important factors involved in visual processing that are present when natural stimuli are used. Technological advancement in stimulus generation and data analysis provide the opportunity to study the ECRF and the CRF in greater detail. Coupled with the growing appreciation of the importance of conscious influence on early sensory processing, the field could see a shift toward using natural stimuli in awake animals for a fuller understanding of the visual system. Despite the tremendous advances in the half-century since Hubel and Wiesel's initial work, there remains much left to learn about the early visual pathway.

Acknowledgments

Abbreviations

CRF	classical receptive field
EC	extra-classical
ECI	extra-classical inhibition
ECRF	extra-classical receptive field
K	koniocellular
LGN	lateral geniculate nucleus
M	magnocellular
MID	Maximally Informative Dimensions
P	Parvocellular
RF	receptive field
RGC	retinal ganglion cell
STA	spike-triggered average
STC	spike-triggered covariance

| **V1** | primary visual cortex |

References

Alitto HJ, Moore BD, Rathbun DL, Usrey WM. A comparison of visual responses in the lateral geniculate nucleus of alert and anaesthetized macaque monkeys. J Physiol. 2011; 589:87–99. [PubMed: 20603332]

Alitto HJ, Usrey WM. Origin and dynamics of extraclassical suppression in the lateral geniculate nucleus of the macaque monkey. Neuron. 2008; 57:135–146. [PubMed: 18184570]

Alivisatos AP, Chun M, Church GM, Greenspan RJ, Roukes ML, Yuste R. The brain activity map project and the challenge of functional connectomics. Neuron. 2012; 74:970–974. [PubMed: 22726828]

Angelucci A, Bressloff PC. Contribution of feedforward, lateral and feedback connections to the classical receptive field center and extra-classical receptive field surround of primate V1 neurons. Prog Brain Res. 2006:93–120.

Babadi B, Casti A, Xiao Y, Kaplan E, Paninski L. A generalized linear model of the impact of direct and indirect inputs to the lateral geniculate nucleus. J Vis. 2010; 10(22):1–14.

Bair W, Cavanaugh JR, Smith MA, Movshon JA. The timing of response onset and offset in macaque visual neurons. J Neurosci. 2002; 22:3189–3205. [PubMed: 11943820]

Baker CL, Cynader MS. Spatial receptive-field properties of direction-selective neurons in cat striate cortex. J Neurophysiol. 1986; 55:1136–1152. [PubMed: 3734852]

Benardete EA, Kaplan E. The receptive field of the primate P retinal ganglion cell, I: linear dynamics. Vis Neurosci. 1997a; 14:169–185. [PubMed: 9057278]

Benardete EA, Kaplan E. The receptive field of the primate P retinal ganglion cell, II: nonlinear dynamics. Vis Neurosci. 1997b; 14:187–205. [PubMed: 9057279]

Bonin V, Mante V, Carandini M. The suppressive field of neurons in lateral geniculate nucleus. J Neurosci. 2005; 25:10844–10856. [PubMed: 16306397]

Bourkiza B, Vurro M, Jeffries A, Pezaris JS. Visual Acuity of Simulated Thalamic Visual Prostheses in Normally Sighted Humans. PLoS ONE. 2013; 8(9):e73592. http://dx.doi.org/10.1371/journal.pone.0073592. [PubMed: 24086286]

Briggman KL, Bock DD. Volume electron microscopy for neuronal circuit reconstruction. Curr Opin Neurobiol. 2012; 22:154–161. [PubMed: 22119321]

Brindley GS, Gautier-Smith PC, Lewin W. Cortical blindness and the functions of the non-geniculate fibres of the optic tracts. J Neurol Neurosurg Psychiatry. 1969; 32:259. [PubMed: 5807867]

Butts DA, Weng C, Jin J, Yeh CI, Lesica NA, Alonso JM, Stanley GB. Temporal precision in the neural code and the timescales of natural vision. Nature. 2007; 449:92–95. [PubMed: 17805296]

Camp AJ, Tailby C, Solomon SG. Adaptable mechanisms that regulate the contrast response of neurons in the primate lateral geniculate nucleus. J Neurosci. 2009; 29:5009–5021. [PubMed: 19369570]

Cheong SK, Tailby C, Solomon SG, Martin PR. Cortical-like receptive fields in the lateral geniculate nucleus of marmoset monkeys. J Neurosci. 2013; 33:6864–6876. [PubMed: 23595745]

Chichilnisky EJ. A simple white noise analysis of neuronal light responses. Netw Comput Neural Syst. 2001; 12:199–213.

Cleland BG, Dubin MW, Levick WR. Simultaneous recording of input and output of lateral geniculate neurones. Nature New Biol. 1971; 231:191–192. [PubMed: 4325715]

Conley M, Fitzpatrick D. Morphology of retinogeniculate axons in the macaque. Vis Neurosci. 1989; 2:287–296. [PubMed: 2562150]

Cottaris NP, De Valois RL. Temporal dynamics of chromatic tuning in macaque primary visual cortex. Nature. 1998; 395:896–900. [PubMed: 9804422]

DeAngelis GC, Ohzawa I, Freeman RD. Receptive-field dynamics in the central visual pathways. Trends Neurosci. 1995; 18:451–458. [PubMed: 8545912]

Derrington AM, Lennie P. Spatial and temporal contrast sensitivities of neurones in lateral geniculate nucleus of macaque. J Physiol. 1984; 357:219–240. [PubMed: 6512690]

Dreher B, Cottee LJ. Visual receptive-field properties of cells in area 18 of cat's cerebral cortex before and after acute lesions in area 17. J Neurophysiol. 1975; 38:735–750. [PubMed: 1159462]

Fairhall A, Shea-Brown E, Barreiro A. Information theoretic approaches to understanding circuit function. Curr Opin Neurobiol. 2012; 22:653–659. [PubMed: 22795220]

Field DJ, Tolhurst DJ. The structure and symmetry of simple-cell receptive-field profiles in the cat's visual cortex. Proc R Soc Lond B Biol Sci. 1986; 228:379– 400. [PubMed: 2877464]

Fitzpatrick D. Seeing beyond the receptive field in primary visual cortex. Curr Opin Neurobiol. 2000; 10:438–443. [PubMed: 10981611]

Goodale MA, Milner AD. Separate visual pathways for perception and action. Trends Neurosci. 1992; 15:20–25. [PubMed: 1374953]

Guimaraes A, Zaremba S, Hockfield S. Molecular and morphological changes in the cat lateral geniculate nucleus and visual cortex induced by visual deprivation are revealed by monoclonal antibodies Cat-304 and Cat-301. J Neurosci. 1990; 10:3014–3024. [PubMed: 1697900]

Haider B, Häusser M, Carandini M. Inhibition dominates sensory responses in the awake cortex. Nature. 2013; 493:97–100. [PubMed: 23172139]

Hamos JE, Van Horn SC, Raczkowski D, Sherman SM. Synaptic circuits involving an individual retinogeniculate axon in the cat. J Comp Neurol. 1987; 259:165–192. [PubMed: 3584556]

Hendry SH, Reid RC. The koniocellular pathway in primate vision. Annu Rev Neurosci. 2000; 23:127–153. [PubMed: 10845061]

Hubel DH, Wiesel TN. Receptive fields of single neurones in the cat's striate cortex. J Physiol. 1959; 148:574–591. [PubMed: 14403679]

Hubel DH, Wiesel TN. Integrative action in the cat's lateral geniculate body. J Physiol. 1961; 155:385–398. [PubMed: 13716436]

Hubel DH, Wiesel TN. Receptive fields, binocular interaction and functional architecture in the cat's visual cortex. J Physiol. 1962; 160:106. [PubMed: 14449617]

Jacobs GH. Primate color vision: a comparative perspective. Vis Neurosci. 2008; 25:619–633. [PubMed: 18983718]

Kaplan E, Purpura K, Shapley RM. Contrast affects the transmission of visual information through the mammalian lateral geniculate nucleus. J Physiol. 1987; 391:267–288. [PubMed: 2832591]

Krüger J. Stimulus dependent colour specificity of monkey lateral geniculate neurones. Exp Brain Res. 1977; 30:297–311. [PubMed: 413725]

Kuffler SW. Discharge patterns and functional organization of mammalian retina. J Neurophysiol. 1953; 16:37–68. [PubMed: 13035466]

Lamme VA, Zipser K, Spekreijse H. Figure-ground activity in primary visual cortex is suppressed by anesthesia. Proc Natl Acad Sci. 1998; 95:3263–3268. [PubMed: 9501251]

Lee BB, Virsu V, Creutzfeldt OD. Linear signal transmission from prepotentials to cells in the macaque lateral geniculate nucleus. Exp Brain Res. 1983; 52:50–56. [PubMed: 6313418]

Lesica NA, Stanley GB. Encoding of natural scene movies by tonic and burst spikes in the lateral geniculate nucleus. J Neurosci. 2004; 24:10731–10740. [PubMed: 15564591]

Levitt JB, Schumer RA, Sherman SM, Spear PD, Movshon JA. Visual response properties of neurons in the LGN of normally reared and visually deprived macaque monkeys. J Neurophysiol. 2001; 85:2111–2129. [PubMed: 11353027]

Mante V, Bonin V, Carandini M. Functional mechanisms shaping lateral geniculate responses to artificial and natural stimuli. Neuron. 2008; 58:625–638. [PubMed: 18498742]

Marmarelis, PZ., Marmarelis, VZ. Computers in Biology and Medicine. Plenum Press; New York: 1978. Analysis of Physiological Systems: The White-Noise Approach.

Martin PR, White AJR, Goodchild AK, Wilder HD, Sefton AE. Evidence that blue-on cells are part of the third geniculocortical pathway in primates. Eur J Neurosci. 1997; 9:1536–1541. (WHERE IS PDF?). [PubMed: 9240412]

Maunsell JH, Ghose GM, Assad JA, McAdams CJ, Boudreau CE, Noerager BD. Visual response latencies of magnocellular and parvocellular LGN neurons in macaque monkeys. Vis Neurosci. 1999; 16:1–14. [PubMed: 10022474]

McMahon MJ, Lankheet MJM, Lennie P, Williams DR. Fine structure of parvocellular receptive fields in the primate fovea revealed by laser interferometry. J Neurosci. 2000; 20:2043–2053. [PubMed: 10684905]

Niell CM, Stryker MP. Modulation of visual responses by behavioral state in mouse visual cortex. Neuron. 2010; 65:472–479. [PubMed: 20188652]

Norton TT, Casagrande VA. Laminar organization of receptive-field properties in lateral geniculate nucleus of bush baby (*Galago crassicaudatus*). J Neurophysiol. 1982; 47:715–741. [PubMed: 6279794]

O'Connor DH, Fukui MM, Pinsk MA, Kastner S. Attention modulates responses in the human lateral geniculate nucleus. Nat Neurosci. 2002; 5(11):1203– 1209. [PubMed: 12379861]

O'Keefe LP, Levitt JB, Kiper DC, Shapley RM, Movshon JA. Functional organization of owl monkey lateral geniculate nucleus and visual cortex. J Neurophysiol. 1998; 80:594–609. [PubMed: 9705453]

Palmer LA, Davis TL. Receptive-field structure in cat striate cortex. J Neurophysiol. 1981; 46:260–276. [PubMed: 6267213]

Pezaris JS, Eskandar EN. Getting signals into the brain: visual prosthetics through thalamic microstimulation. Neurosurg Focus. 2009; 27:E6.

Pezaris JS, Reid RC. Demonstration of artificial visual percepts generated through thalamic microstimulation. Proc Natl Acad Sci. 2007; 104:7670–7675. [PubMed: 17452646]

Reid RC, Shapley RM. Space and time maps of cone photoreceptor signals in macaque lateral geniculate nucleus. J Neurosci. 2002; 22:6158–6175. [PubMed: 12122075]

Reid RC, Victor JD, Shapley RM. The use of m-sequences in the analysis of visual neurons: linear receptive field properties. Vis Neurosci. 1997; 14:1015–1027. [PubMed: 9447685]

Reinagel P, Reid RC. Temporal coding of visual information in the thalamus. J Neurosci. 2000; 20:5392–5400. [PubMed: 10884324]

Reppas JB, Usrey WM, Reid RC. Saccadic eye movements modulate visual responses in the lateral geniculate nucleus. Neuron. 2002; 35:961–974. [PubMed: 12372289]

Ringach D, Shapley R. Reverse correlation in neurophysiology. Cogn Sci. 2004; 28:147–166.

Roorda A. Adaptive optics for studying visual function: a comprehensive review. J Vis. 2011; 11:6.

Saul AB. Effects of fixational saccades on response timing in macaque lateral geniculate nucleus. Vis Neurosci. 2010:1–11. [PubMed: 20392301]

Sceniak MP, Chatterjee S, Callaway EM. Visual spatial summation in macaque geniculocortical afferents. J Neurophysiol. 2006; 96:3474–3484. [PubMed: 16928793]

Sceniak MP, Ringach DL, Hawken MJ, Shapley R. Contrast's effect on spatial summation by macaque V1 neurons. Nat Neurosci. 1999; 2:733–739. [PubMed: 10412063]

Shapley R, Perry VH. Cat and monkey retinal ganglion cells and their visual functional roles. Trends Neurosci. 1986; 9:229–235.

Sharpee TO. Computational identification of receptive fields. Annu Rev Neurosci. 2013; 36:103–120. [PubMed: 23841838]

Simoncelli EP. Vision and the statistics of the visual environment. Curr Opin Neurobiol. 2003; 13:144–149. [PubMed: 12744966]

Simoncelli EP, Olshausen BA. Natural image statistics and neural representation. Annu Rev Neurosci. 2001; 24:1193–1216. [PubMed: 11520932]

Sincich LC, Horton JC, Sharpee TO. Preserving information in neural transmission. J Neurosci. 2009a; 29:6207–6216. [PubMed: 19439598]

Sincich LC, Zhang Y, Tiruveedhula P, Horton JC, Roorda A. Resolving single cone inputs to visual receptive fields. Nat Neurosci. 2009b; 12:967–969. [PubMed: 19561602]

Solomon SG, Lee BB, Sun H. Suppressive surrounds and contrast gain in magnocellular-pathway retinal ganglion cells of macaque. J Neurosci. 2006; 26:8715–8726. [PubMed: 16928860]

Solomon SG, Lennie P. The machinery of colour vision. Nat Rev Neurosci. 2007; 8:276–286. [PubMed: 17375040]

Solomon SG, Tailby C, Cheong SK, Camp AJ. Linear and nonlinear contributions to the visual sensitivity of neurons in primate lateral geniculate nucleus. J Neurophysiol. 2010; 104:1884–1898. [PubMed: 20685925]

Solomon SG, White AJ, Martin PR. Extraclassical receptive field properties of parvocellular, magnocellular, and koniocellular cells in the primate lateral geniculate nucleus. J Neurosci. 2002; 22:338–349. [PubMed: 11756517]

Stanley GB, Li FF, Dan Y. Reconstruction of natural scenes from ensemble responses in the lateral geniculate nucleus. J Neurosci. 1999; 19:8036–8042. [PubMed: 10479703]

Stevens JK, Gerstein GL. Interactions between cat lateral geniculate neurons. J Neurophysiol. 1976; 39:239–256. [PubMed: 1255221]

Sutter EE. The fast m-transform: a fast computation of cross-correlations with binary m-sequences. SIAM J Comput. 1991; 20:686–694.

Tailby C, Szmajda BA, Buzás P, Lee BB, Martin PR. Transmission of blue (S) cone signals through the primate lateral geniculate nucleus. J Physiol. 2008; 586:5947–5967. [PubMed: 18955378]

Talebi V, Baker CL. Natural versus synthetic stimuli for estimating receptive field models: a comparison of predictive robustness. J Neurosci. 2012; 32:1560–1576. [PubMed: 22302799]

Tan Z, Yao H. The spatiotemporal frequency tuning of LGN receptive field facilitates neural discrimination of natural stimuli. J Neurosci. 2009; 29:11409– 11416. [PubMed: 19741147]

Uhl RR, Squires KC, Bruce DL, Starr A. Effect of halothane anesthesia on the human cortical visual evoked response. Anesthesiology. 1980; 53:273–276. [PubMed: 7425354]

Ungerleider L, Mishkin M. Two cortical visual systems. Anal Vis Behav. 1982:549–586.

Usrey WM, Reid RC. Visual physiology of the lateral geniculate nucleus in two species of New World monkey: *Saimiri sciureus* and *Aotus trivirgatis*. J Physiol. 2000; 523:755–769. [PubMed: 10718753]

Victor JD, Knight BW. Nonlinear analysis with an arbitrary stimulus ensemble. Q Appl Math. 1979:113–136.

Webb BS, Tinsley CJ, Barraclough NE, Easton A, Parker A, Derrington AM. Feedback from V1 and inhibition from beyond the classical receptive field modulates the responses of neurons in the primate lateral geniculate nucleus. Vis Neurosci. 2002; 19:583–592. [PubMed: 12507325]

Webb BS, Tinsley CJ, Vincent CJ, Derrington AM. Spatial distribution of suppressive signals outside the classical receptive field in lateral geniculate nucleus. J Neurophysiol. 2005; 94:1789–1797. [PubMed: 15888523]

White AJ, Solomon SG, Martin PR. Spatial properties of koniocellular cells in the lateral geniculate nucleus of the marmoset *Callithrix jacchus*. J Physiol. 2001; 533:519–535. [PubMed: 11389209]

Wiesel TN, Hubel DH. Spatial and chromatic interactions in the lateral geniculate body of the rhesus monkey. J Neurophysiol. 1966; 29:1115–1156. [PubMed: 4961644]

Xu X, Ichida JM, Allison JD, Boyd JD, Bonds AB, Casagrande VA. A comparison of koniocellular, magnocellular and parvocellular receptive field properties in the lateral geniculate nucleus of the owl monkey (*Aotus trivirgatus*). J Physiol. 2001; 531:203–218. [PubMed: 11179404]
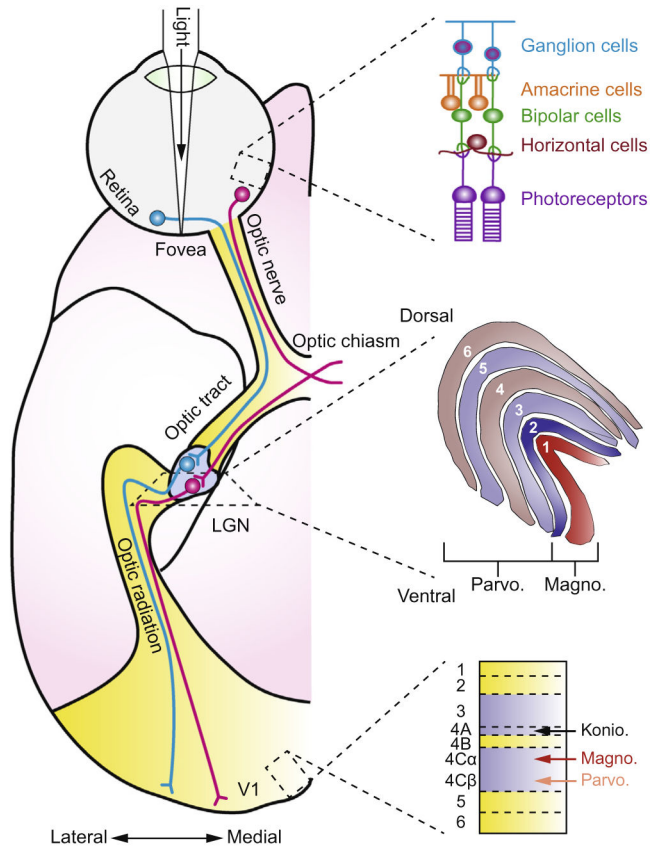
Fig. 1.

Early visual system pathways of the macaque monkey. The figure on the left shows the pathway of visual information imaged on the retina as it passes through the LGN and arrives at the primary visual cortex (V1). The anatomical schematic represents a ventral view of the right hemisphere. The visual scene is imaged by photoreceptors in the retina and information is passed through bipolar cells to retinal ganglion cells whose axons exit the back of the eyeball forming the optic nerve. Information from the contralateral part of the scene reaches the LGN with input from the two eyes arriving at separate layers of the LGN: layers 2, 3, and 5 receive input from the ipsilateral eye and layers 1, 4, and 6 receive input from the contralateral eye. The magnocellular layers (1 and 2) receive input that originated from rod photoreceptors and the Parvocellular layers (3–6) receive input that originated from cone photoreceptors. Koniocellular cells in the LGN are interspersed between the magnocellular and parvocellular layers and receive information arising from short-wavelength cones. Cells in the LGN project mainly to layer 4 of the primary visual cortex through a formation called the optic radiation. Adapted from Solomon and Lennie, 2007 with permission.
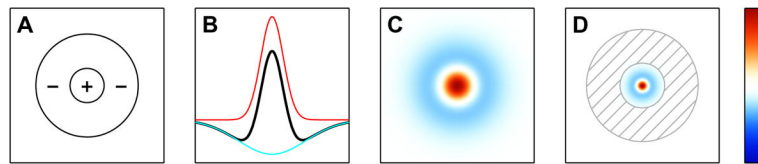
Fig. 2.
Classical and Extra-Classical Receptive Fields in the LGN. (A) The classical receptive field (CRF) comprises a central *on* or *off* region and a surrounding ring having the opposite sign. For *on*-center cells, light in the center excites the cell and light in the surround inhibits the cell; the reverse is true for *off*-center cells. Firing rate is approximately linearly determined by weighting the light in the center and surround regions. (B) The CRF can be modeled as the sum of two Gaussians, shown in section through the center of the field, a narrower excitatory region shown in red and a broader inhibitory one shown in blue for the example *on* cell here. The sum of the two is in black, and forms the well-known Mexican Hat profile. (C) The same difference of Gaussians is shown in a full two dimensional plot where color ranges from deep red for excitatory, through white for indifferent, and deep blue for inhibitory. Since the inhibitory field is not as strong as the excitatory field, it does not reach into deep blues, but remains at lighter ones. (D) The ECRF is an as-yet poorly defined region that is larger than the CRF, and is shown here in hatched gray. The reader should note that the ECRF may also extend through the area of visual space in which the CRF resides. Stimuli in the ECRF modulate the response to stimuli in the CRF, but without being able to directly generate spikes. Current thought holds that the ECRF provides contrast-dependent gain control on CRF sensitivity.
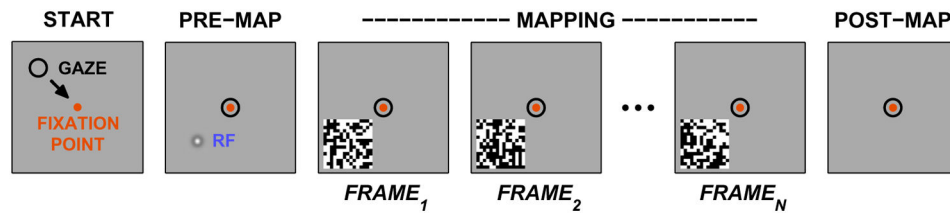
Fig. 3.

Typical Mapping Paradigm. The standard mapping paradigm used to measure response fields (RFs) in primates places a computer monitor at a fixed distance in front of the subject and displays mapping stimuli while neural signals are recorded. Experiments include a sequence of phases that are presented in order, as shown in this figure. Prior to stimulus presentation, the gaze is localized to a known point on the screen (PRE-MAP) which will also bring the putative RF of the cell under study to a known location, relative to the fixation point. A series of mapping stimuli, depicted here as a set of black-and-white random checkerboards, is then shown as the neural response is captured (MAPPING). Often a brief quiet period is included after the stimulus ends before the recording concludes (POST-MAP). For awake preparations especially, the Mapping phase can be brief, and the sequence repeated many times with different temporal segments of the mapping stimuli to build up an aggregate set of data. When the location of the RF is not known a-priori, a sequence of mappings can be made that starts with checkerboards with large squares, and progresses to finer checkerboards, spanning progressively smaller portions of the visual field while providing increasingly fine detail. Complete mapping of an RF may require many thousands of checkerboard frames, although a single set of frames is often re-used from one neuron to the next.
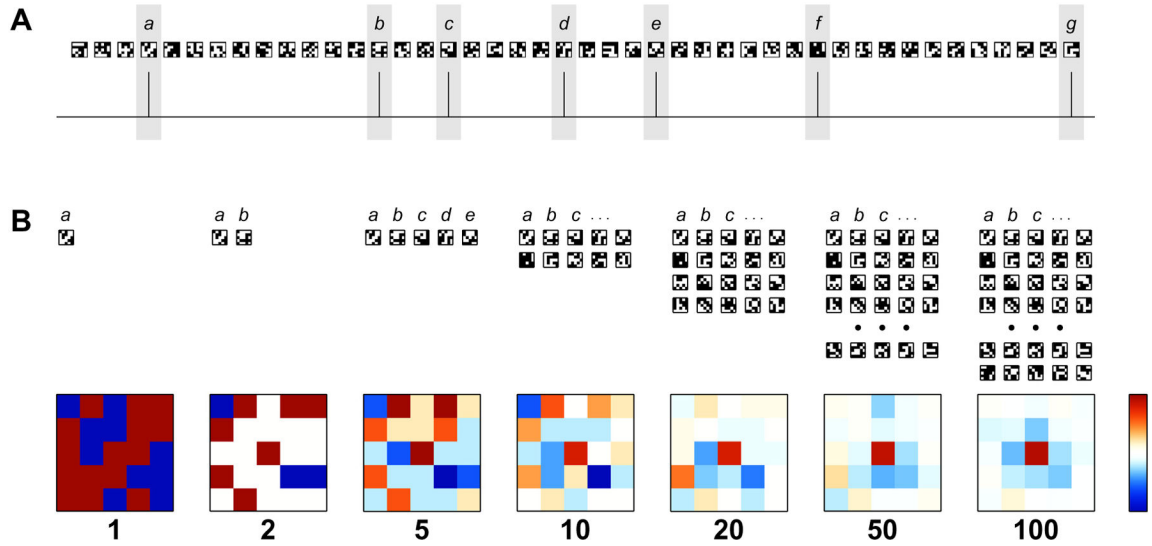
Fig. 4.

RF Extraction via Spike Triggered Averaging. The simplest methods to compute the RF from a recording use the Spike Triggered Averaging (STA) technique. This method and its variants rely upon the independence between signal and noise, and presume that at any given instance that the cell responds by firing a spike, there is some commonality among the stimuli presented that have elicited each spike. The commonality is interpreted as being descriptive of the linear portion of the RF, whereas non-commonalities in the stimuli will tend to average to zero for well-constructed stimuli. (A) A sequence of 5-by-5 checkerboards in temporal order along with an extracted spike train. Stimuli of practical use have many more squares than the reduced version shown here. Frames where a spike was detected are highlighted with a light gray box and labeled with lower case letters starting with *a*. (B) Labeled frames are collected, averaged, and normalized to form a map, shown here in snapshots with 1, 2, 5, etc. spikes detected to depict the evolution of the computation with an according number of checkerboards. Maps are shown on a scale where deep red represents response to white squares of the checkerboard, white indicates indifference to the stimulus, and deep blue represents response to black squares of the checkerboard. The map that is computed depicts the response of an *on*-center cell. Not shown is the extension of this technique to examine frames that immediately preceded each spike: the computation is run multiple times with differing temporal offsets between spike and selected frames, generating a movie of the optimal stimulus.